NASA Technical Memorandum 82924

NASA-TM-82924 19820024206

Rough Analysis of Installation Effects on Turboprop Noise

Paul A. Durbin and John F. Groeneweg
Lewis Research Center
Cleveland, Ohio

Prepared for the
One hundred fourth Meeting of the Acoustical Society of America
Orlando, Florida, November 8-12, 1982

NASA

ERRATA

NASA Technical Memorandum 82924

ROUGH ANALYSIS OF INSTALLATION EFFECTS
ON TURBOPROP NOISE

Paul A. Durbin and John F. Groeneweg
November 1982

Page 2: The second line of equation (1) should read

$$x\left[\frac{T_p}{T_0}\left(\cos\theta - \frac{B-p}{k_B r_M}\operatorname{cotan} x\right) + i\delta_0^p \frac{B\rho_o a_o^2 h M_r c_b s_b}{r_M T_0}\right] \qquad (1)$$

Page 4: Equation (4) should read

$$\underset{\sim}{u} = (U + u'(x, r_M \sin \Omega t), V + v'(x, r_M \sin \Omega\tau) + \Omega r_M \cos \Omega t, -\Omega r_M \sin \Omega t)$$

Page 4: Equation (5) should read

$$\underset{\sim}{u} \cdot \underset{\sim}{n} = -U \sin x + V \cos x \cos \Omega t - \Omega r_M \cos x - u'(x, r_M \sin \Omega t)\sin x$$

$$+ v'(x, r_M \sin \Omega t)\cos x \cos \Omega t$$

Page 4: The first of equations (8) should read

$$(\underset{\sim}{u} \cdot \underset{\sim}{n})_1 = (\underset{\sim}{u} \cdot \underset{\sim}{n})_{-1} = \left(U \cos x \sin \alpha\right)/2$$

Page 5: On the right side of equation (9), the denominator should read

$$2\pi\left(x_o^2 + r_M^2 \sin^2\tau\right)$$

Page 5: On the right side of the second equation, the first fraction should be

$$\frac{\kappa}{(2\pi)^2}$$

Page 5: On the right side of the fourth equation, the denominator of the integrand should be

$$r_M^2 y^2 - \left(2r_M^2 + 4x_o^2\right)y + r_M^2$$

Page 5: The fifth equation should read

$$\underset{-}{a_+} = 1 + 2x_o^2/r_M^2 \pm 2x_o/r_M\sqrt{1 + x_o^2/r_M^2}$$

Page 6: Equation (12) should read

$$\frac{\pi M_x M_r a_0^2 c_b s_b}{T_0/\rho_0 \tan x}(\sin \alpha)/2 \approx 25(\sin \alpha)/2$$

ROUGH ANALYSIS OF INSTALLATION EFFECTS ON TURBOPROP NOISE

Paul A. Durbin and John F. Groeneweg

National Aeronautics and Space Administration
Lewis Research Center
Cleveland, Ohio 44135

SUMMARY

A rough analysis of noise from a propeller operated at angle of attack, and in the nonuniform flow due to a line vortex approximating a wing flow field suggests installation can significantly affect turboprop noise levels. On one side of the propeller, where the blades approach the horizontal plane from above, decreases of noise occur; while on the other side noise increases. The noise reduction is due to negative interference of steady and unsteady sources. An angle of attack, or distance between propeller and vortex, exists for which noise is a minimum.

INTRODUCTION

A drawback to use of the turboprop as an efficient means of aircraft propulsion is the fact that it may produce considerable noise - particularly within the cabin, as well as in the community. This has spurred research into turboprop noise sources. Operating in a uniform axial flow, noise is associated with forces on blades and flow disturbances which are steady in the blade frame of reference. However, when installed on a wing the propeller will operate at an angle to its inflow, which is also spatially nonuniform, due to the mean flow around the wing and the engine nacelle. This flow nonuniformity produces unsteady blade forces, which contribute to the noise field. Preliminary experimental investigations of installation effects, made by Dittmar and Jeracki (Ref. 1) and by Tanna, et al. (Ref. 2), show that substantial noise increases can result.

The relative importance of unsteady noise sources is determined both by the unsteady aerodynamic response of the propeller blades and by the efficiency with which the resulting unsteady blade forces radiate acoustic disturbances. The purpose of this report is to give a rough analysis of the effect of inflow angle and wing induced installation effects on turboprop noise. We will find the unsteady noise source to be comparable to, and sometimes significantly larger than, the steady source. It is hoped that the present crude analysis will provide an impetus for more elaborate theoretical and experimental investigations of this subject.

SYMBOLS

a_0	sound speed
B	number of blades
c_b	blade chord
h	thickness of blade
J_n	Bessel function of order n
k_B	$B\Omega / a_0$
L	lift on wing
M_r, M_x	Mach number of flow relative to blade and in axial direction
M_θ	circumferential Mach number of blade

N_e	number of engines
P_B	acoustic pressure at blade passing frequency
p	harmonic number of blade force
r_M	radius at 3/4 span
s_b, s_w	blade and wing span
T_p, T_0	p^{th} harmonic of thrust, steady thrust per blade
t	time
u, v	axial and transverse velocity
u_f	flight velocity
w_p	defined below Eq. (10)
x, y	cartesian coordinates, see fig. 1
x_0	distance from prop plane to wing 1/4 chord; fig. 1
α	angle of attack
θ, φ	spherical polar coordinates, see fig. 1
κ	wing circulation
ρ_0	density of air
σ_1	$pc_bM_\theta/2M_r r_M$
τ	Ωt
χ	blade stagger angle
Ω	propeller angular velocity

ANALYTICAL MODEL

A simple model for noise radiated by a propeller with unsteady loading, due to Lowson, is described in section 3.5.3 of Ref. 3. In this model each loaded propeller blade is represented by a rotating point force. We will take this force to be situated at 3/4 of the blade span. Hawking and Lowson (Ref. 4) added a term accounting for thickness noise to Lowson's model; to a first approximation thickness only contributes to steady noise. With this term incorporated, the acoustic pressure radiated at the blade-passing frequency is given by (see Eq. (3.119) of Ref. 3)

$$P_B = \frac{ik_B B T_0 N_e^{1/2}}{4\pi x} e^{i(k_B x + B\varphi)} \sum_{p=-\infty}^{\infty} e^{-ip\varphi} J_{B-p}(k_B r_M \sin\theta)$$

$$\times \left[\frac{T_p}{T_0} \left(\cos\theta - \frac{B-p}{k_B r_M} \operatorname{cotan} \chi \right) + i\delta_0^p \frac{B\rho_0 a_0^2 h M_r c_b s_b}{r_M T_0} \right] \qquad (1)$$

Errata 1-11-85

where $\delta_0^p = 1$ if $p = 0$, and $\delta_0^p = 0$ if $p \neq 0$. This expression assumes noise is due to radiation from N_e uncorrelated engines. Symbols are defined in the symbol list and the angle φ is the angle in the propeller plane - the plane of the wing being $\varphi = \pm\pi/2$. θ is 0 in front of the propeller, $\pm\pi/2$ in the propeller plane, and π in back of the propeller (see Fig. 1).

The factor in front of the summation in Eq. (1) can be ignored, since we are concerned only with the relative importance of steady and unsteady contributions to $|P_B|^2$. The relative strengths of these contributions depends on T_p/T_0. This ratio is estimated below for two cases: a propeller operated at a small angle of attack to a uniform flow, and a propel-

ler operated in the upwash due to a point vortex; the latter being a crude representation of a lifting airfoil. We must also estimate the relative contribution of thickness noise, as represented by the last term in square brackets in Eq. (1).

Thickness Noise

Table I lists values which have been used in our analysis. These are representatives of the SR-3 turboprop at design conditions, and at 3/4 span. Obviously it is quite an approximation to replace a blade with such an intricate geometry as that of the SR-3 (Fig. 1) by a representative point. However, it must suffice for our present "back of the envelope" analysis. We define a thickness parameter by

$$\text{THICK} \equiv B\rho_0 a_0^2 h M_r c_b s_b / r_M T_0$$

The magnitude of this term increases with B; for the typical eight or ten-bladed propeller under flight conditions, thickness is comparable to loading. Substituting values from Table I gives THICK = 1.7 for B = 8.

Unsteady Force

To determine the p^{th} harmonic of the unsteady thrust, T_p, we require the p^{th} harmonic of the upwash on the propeller blade and the aerodynamic response function of the blade. For the latter, we use the approximate compressible Sears function (Ref. 3, Eq. (3.70) with obvious modification).

$$\frac{T_p}{T_0} = \pi\rho_0 (\underset{\sim}{u} \cdot \underset{\sim}{n})_p M_r a_0 c_b s_b \frac{\sin \chi}{T_0} S_c(\sigma_1, M_r) \tag{2}$$

with

$$S_c = \frac{e^{i(\pi/4 - \sigma_1)}}{\sigma_1 \pi} \sqrt{\frac{2}{M_r}} \mathcal{F}\left(\sqrt{\frac{4\sigma_1 M_r}{\pi(1 + M_r)}}\right)$$

where $\mathcal{F}$ is the complex Fresnel integral. Here $(\underset{\sim}{u} \cdot \underset{\sim}{n})_p$ is the p^{th} harmonic of the velocity normal to the blade, in the blade frame of reference. $\underset{\sim}{n}$, the normal to the blade referred to fixed coordinate axes, is

$$\underset{\sim}{n} = (-\sin \chi, \cos \chi \cos \Omega t, \cos \chi \sin \Omega t) \tag{3}$$

We consider a two-dimensional velocity field

$$\underset{\sim}{u} = (U + u'(x, r_M \cos \varphi)V + v'(x, r_M \cos \varphi), 0)$$

having substituted the value $y = r_M \cos \varphi$ at the 3/4 chord. Also, x is the axial coordinate perpendicular to the propeller plane (see Fig. 1).

In the propeller frame $\varphi = \Omega t - \pi/2$ (the initial phase of $-\pi/2$ is required for consistency with Eq. (1)) and

$$\underset{\sim}{u} = (U + u'(x, r_M \sin \Omega t), V + v'(x, r_M \sin \Omega\tau) + \Omega r_M \cos \Omega t, -\Omega r_M \sin \Omega t) \quad (4)$$

Errata 6-11-85

Thus

$$\underset{\sim}{u} \cdot \underset{\sim}{n} = -U \sin \chi + V \cos \chi \cos \Omega t - \Omega r_M \cos \chi - u'(x, r_M \sin \Omega t)\sin \chi$$

$$+ v'(x, r_M \sin \Omega t)\cos \chi \cos \Omega t \quad (5)$$

We require only the unsteady part of Eq. (5):

$$\underset{\sim}{u} \cdot \underset{\sim}{n} = V \cos \chi \cos \Omega t - u'(x, r_M \sin \Omega t)\sin \chi + v'(x, r_M \sin \Omega t)\cos \chi \cos \Omega t \quad (6)$$

The p^{th} harmonic of this, which appears in Eq. (2), is

$$(\underset{\sim}{u} \cdot \underset{\sim}{n})_p = \frac{1}{2\pi} \int_0^{2\pi} e^{ip\tau} (\underset{\sim}{u} \cdot \underset{\sim}{n})(\tau) d\tau \quad (7)$$

where

$$\tau = \Omega t$$

Propeller at Angle of Attack

If the flow is spatially uniform, $u' = v' = 0$; and if the propeller is at angle of attack, α, $V = (U/\cos \alpha)\sin \alpha$. If α is small the axial Mach number into the propeller, $U/\cos \alpha$, may be taken to be U. In this case, obviously

Errata 6-11-85

$$\left.\begin{aligned} (\underset{\sim}{u} \cdot \underset{\sim}{n})_1 = (\underset{\sim}{u} \cdot \underset{\sim}{n})_{-1} &= \left(U \cos \chi \sin \alpha\right)/2 \\ (\underset{\sim}{u} \cdot \underset{\sim}{n})_p &= 0, \quad |p| \neq 1 \end{aligned}\right\} \quad (8)$$

Vortex Flow

At zero angle of attack $V = 0$. Then unsteady forces are produced by u' and v' alone. An installed turboprop will be operating in the potential flow around a lifting wing. To roughly estimate the effect of this source of flow perturbation, we consider the effect on noise production of a line vortex, a distance x_0 downstream of the propeller plane.

For the line vortex

$$(u', v') = \kappa(-y, x)/2\pi(x^2 + y^2)$$

At $x = x_0$, $y = r_M \sin \tau$, and with $\underset{\sim}{n}$ given by Eq. (3)

Errata 6-11-85

$$(\underset{\sim}{u}' \cdot \underset{\sim}{n}) = \frac{\kappa(r_M \sin\chi \sin\tau + x_o \cos\chi \cos\tau)}{2\pi\left(x_o^2 + r_M^2 \sin^2\tau\right)} \tag{9}$$

Then

$$(\underset{\sim}{u}' \cdot \underset{\sim}{n})_p \frac{\kappa}{(2\pi)^2} \int_0^{2\pi} \frac{e^{ip\tau}(r_M \sin\chi \sin\tau + x_o \cos\chi \cos\tau)}{x_o^2 + r_M^2 \sin^2\tau} d\tau$$

or, integrating around the unit circle

$$(\underset{\sim}{u}' \cdot \underset{\sim}{n})_p = \frac{\kappa}{2\pi^2} \oint \frac{z^p[(r_M \sin\chi + ix_o \cos\chi)z^2 - (r_M \sin\chi - ix_o \cos\chi)]}{r_M^2 z^4 - \left(2r_M^2 + 4x_o^2\right)z^2 + r_M^2} dz$$

This is equal to zero if p is even. If $p = 2n + 1$ and $y = z^2$

$$(\underset{\sim}{u}' \cdot \underset{\sim}{n})_p = \frac{\kappa}{2\pi^2} \oint \frac{y^n[(r_M \sin\chi + ix_o \cos\chi)y - (r_M \sin\chi - ix_o \cos\chi)]}{r_M^2 y^2 - \left(2r_M^2 + 4x_o^2\right)y + r_M^2} dy$$

This has poles at

$$a_{\pm} = 1 + 2x_o^2/r_M^2 \pm 2x_o/r_M \sqrt{1 + x_o^2/r_M^2}$$

but only a_- is inside the contour of integration. Thus, evaluating the residue

$$(\underset{\sim}{u}' \cdot \underset{\sim}{n})_{2n+1} = \frac{\kappa}{2\pi r_M}\left\{\frac{2ia_-^n[(\sin\chi + ix_o/r_M \cos\chi)a_- - (\sin\chi - ix_o/r_M \cos\chi)]}{a_- - a_+}\right\} \tag{10}$$

For later use, we define $w_p(\chi, x_o/r_M)$ as the factor in curly brackets when $p = 2n + 1$ and $w_p = 0$ when $p = 2n$.

Estimates for Factors Determining Relative Strengths of Unsteady Forces

Returning to Eqs. (1) and (2), we find

$$\frac{T_p}{T_0} = \left[\frac{\pi(\underset{\sim}{u} \cdot \underset{\sim}{n})_p M_r a_0 c_b s_b}{T_0/\rho_o \sin\chi}\right] S_c \tag{11}$$

The term in brackets is the ratio of unsteady-to-steady force normal to the blade surface, when $S_c = 1$.

For the propeller at angle of attack, the bracketed factor is

Errata 6-11-85

$$\frac{\pi M_x M_r a_0^2 c_b s_b}{T_0/\rho_0 \tan \chi} (\sin \alpha)/2 \approx 25(\sin \alpha)/2 \qquad (12)$$

for $p = \pm 1$, using the parameter values in Table I. Admittedly, the value of 25 for the bracketed term in Eq. (12) involves severe approximations, and it might be profitable to regard the entire bracketed term as a parameter ranging between 10 and 100, say.

For the vortex flow

$$\frac{T_p}{T_0} = \left[\frac{\kappa M_r a_0 c_b s_b}{2 r_M T_0/\rho_0 \sin \chi}\right] w_p(x, x_0/r_M) S_c$$

If we relate κ to the lift per unit span on the wing by

$$\kappa = L/\rho_0 u_f s_w$$

the bracketed term becomes

$$\text{RATIO} \equiv (L/BT_0) \frac{BM_r s_b c_b}{2M_f s_w r_M} \sin \chi \qquad (13)$$

where L/BT_0 is the lift-to-thrust ratio listed in Table II. This table also gives values of RATIO for potential aircraft configurations and operating conditions estimated from aircraft studies reported in Ref. 5.

RESULTS AND DISCUSSION

The coefficients T_p/T_0 in Eq. (1) decrease rapidly with p while the magnitude of the Bessel functions decrease with $B - p$. Thus, the argument in the summation is small when $p < 0$ (i.e., $B - p > B$) and when $p > B$ if B is sufficiently large. For this reason, to obtain numerical results we have replaced the limits of summation in Eq. (1) by 0 and B. (Of course, for the angle of attack case there are only three non-zero terms, $p = -1, 0, 1$ so truncation is a matter of course.) This truncated version of Eq. (1) was then evaluated for the angle of attack case with the parameters given in Table I, and for the flight cases listed in Table II.

Angle of Attack

The SR-3 turboprop was operated at small angle of attack in a vertical plane in a wind tunnel by Dittmar and Jeracki, and noise measurements were made on the sidewalls. It was found that (at design conditions) on the wall approached from above by the blades (north wall in the experiment) noise increased with angle of attack. On the other wall the noise level remained constant with angle of attack, within the accuracy of measurements: a ten-

dency for noise initially to dip slightly with angle of attack was observed, but this was within the data scatter.

In Fig. 2 we show evaluations of Eq. (1) for angle of attacks of 2° and 4°. This figure shows the directivity pattern, $|P_B|^2$ vs. θ (at fixed radius from the propeller) in the horizontal plane $\varphi = \pm\pi/2$. $\theta = 0$ is directly in front of the propeller and $\theta = \pi$ directly behind; thus, there are troughs in the noise level fore and aft of the propeller and peaks at the sides. The curve for steady loading without the thickness term is in cluded to show the relative contributions of the two terms.

As in the data, noise rises on the side of the propeller where the blades approach the horizontal plane from above. The magnitude of this rise is roughly equal to that measured, although one could not expect the present crude analysis to agree quantitatively with experiment.

On the opposite side of the propeller in the horizontal plane noise drops initially with angle of attack. This may be thought of as a negative interference between unsteady and steady noise components. If one continues to increase the angle of attack, the noise on the side where the blade approaches from below eventually rises. Thus, there is an angle of attack which produces a minimum of noise; this is shown in Fig. 3. The horizontal axis in Fig. 3 is 25 sin α. Thus, if 25 is regarded as a particular value of a variable parameter, the horizontal axis may be regarded as corresponding to different values of this parameter and to different α. Clearly, the larger the value of the parameter, the smaller the α at which minimum noise occurs.

In Fig. 4 we show results corresponding to $\alpha = 4^\circ$ in Fig. 1, but evaluated above and below the propeller in a vertical plane, $\varphi = 0$ and π. Unsteadiness increases noise above and slightly reduces it below the propeller, although the magnitude of the changes are less than in the horizontal plane.

Flight Cases

The aircraft parameters used in our vortex wing model were based on turboprop aircraft studies reported in Ref. 5, and are listed in Table II for a two-engine configuration, operated at takeoff and at cruise. Directivity patterns in the plane of the wing are shown in Fig. 5 for the steady reference and installed cases at propeller-to-wing spacings, x_0/r_M, of 1 and 2. The vortex flow produces both angle of attack and flow non-uniformity at the propeller, and both of these contribute to unsteady noise.

According to Fig. 5 unsteady noise sources are dominant at cruise conditions, while at takeoff they are comparable to steady sources. This is in part due to the larger values of RATIO at cruise and in part due to the smaller value of χ. As in the angle of attack case, there is one side of the propeller (blade approaching wing from below) on which unsteadiness can lead to significant noise reduction. The curves in this figure are referred to an arbitrary level, but the same reference level has been used for takeoff and for cruise. Thus, the steady takeoff noise is about 5 dB higher than at cruise. The value of 5 db is based on the takeoff thrust being six times that at cruise (lapse of six). Some proposed turboprop designs use a smaller lapse. The ratio of noise levels decreases as 20 Ln (lapse); thus for a lapse of three, steady takeoff noise is 1 dB lower than cruise.

As expected, the cases $x_0/r_M = 1$ and $x_0/r_M = 2$ in Fig. 5 indicate that unsteady noise sources decrease in importance as the propeller is moved away from the wing. Figure 6 illustrates further the dependence of

peak noise on x_0/r_M at which noise on one side of the propeller attains a minimum. This x_0/r_M is that for which steady and unsteady sources nearly cancel. At larger x_0/r_M steady sources dominate while at smaller x_0/r_M unsteady sources dominate.

Directivity patterns in the plane of the wing bear on the problem of cabin noise. Community noise is related to noise in the vertical plane below the wing at takeoff conditions. The vertical plane directivity is shown in Fig. 7 for the engine configuration of Table II, with $x_0/r_M = 1$. It can be seen that unsteadiness increases noise both above and below the propeller, although the maximum noise in this plane is less than that in the plane of the wing. Increases in the vertical plane were also obtained at cruise conditions. A polar plot of the fundamental tone directivity in the plane of the propeller, $\theta = \pi/2$, is shown in Fig. 8. Maxima occur at about $\varphi = 20^\circ$ and 160°; minima at about $\varphi = 240^\circ$ and 310°. Increases in tone levels relative to steady loading prevail over half the circle.

Figures 9(a) and (b) present the parametric dependence of peak noise levels in the $\varphi = \pm\pi/2$ plane on THICK and RATIO. Their definitions above Eq. (2) and in Eq. (13) show these parameters to be inversely proportional to steady thrust. Thus, if Fig. 9(a) is interpreted as showing the relative contribution of thickness noise, this contribution increases as steady thrust is reduced at $\varphi = \pi/2$; but initially it may decrease with decreasing thrust at $\varphi = -\pi/2$. The dependence on RATIO is similar to the dependence on α shown in Fig. 3.

CONCLUDING REMARKS

The rough calculations of installation effects on turboprop noise reported here indicate that unsteady sources significantly modify the levels of noise radiated at blade passing frequency. Noise increases of several decibels occur due to both the simple inflow at an angle to the propeller axis (angle of attack) and the more complicated wing upwash flow field, approximated by a line vortex. Asymmetry with respect to the fan axis in the flow field produces an asymmetric acoustic directivity field. In this respect the rough model is in qualitative agreement with the limited experimental results available. Since noise in the plane of the wing goes up on the side for which the blades approach from above and down on the other, the implication is that cabin noise would be lowered by choosing opposite directions of propeller rotation on either side of the fuselage. Whether the tone levels with unsteady sources are actually reduced from the steady values by interference requires further investigation and experimental confirmation. The strong minima exhibited in the calculations are in part a consequence of choosing a single spanwise position to represent the blades. For a spanwise distributed source cancellation between steady and unsteady components would be less complete: a next level of approximation in the analysis would be to sum the contributions from several spanwise strips. In spite of the simplicity of the present analysis, it supports the position that installation effects are an important turboprop noise concern, and suggests this aspect of the problem deserves further investigation.

REFERENCES

1. J. H. Dittmar and R. J. Jeracki, NASA TM-82738, 1981.

2. H. K. Tanna, R. H. Burrin and H. E. Plumble, J. Aircraft 18 (4), 303-309 (1981).

3. M. E. Goldstein, Aeroacoustics (McGraw-Hill, New York, 1976).

4. D. L. Hawkins and M. V. Lowson, J. Sound Vibr. 36 (1) 1-20 (1974).

5. J. C. Muehlbauer, J. G. Hewel, Jr., S. P. Lindenbaum, C. C. Randall, N. Searle, and R. G. Stone, Jr., NASA CR-165813, 1981.

TABLE I. - PARAMETERS FOR SR-3 PROPELLER

AT DESIGN CONDITIONS, 3/4 SPAN

$T_0/\rho_0 = 1.5 \times 10^{10}$ cm^4/s^2
$B = 8$
$M_x = 0.8$
$M_r = 0.97$
$M_\theta = 0.55$
$x = 0.602$
$h = 0.03\ c_b$
$c_b = 0.4\ s_b$
$s_b = 25$ cm
$r_M = 24.8$ cm

TABLE II. - PARAMETERS FOR FLIGHT CASE

$N_e = 2$
$B = 10$
$M_\theta = 0.545$
$c_b/r_M = 0.4$
$s_b/s_w = 0.075$

	Take-off	Cruise
M_r/M_f	2.24	1.2
L/BT_0	6.67	44.
x	$\pi/3$	$\pi/6$
RATIO	1.9	33.6
THICK	0.21	22.1
M_r	0.6	0.97

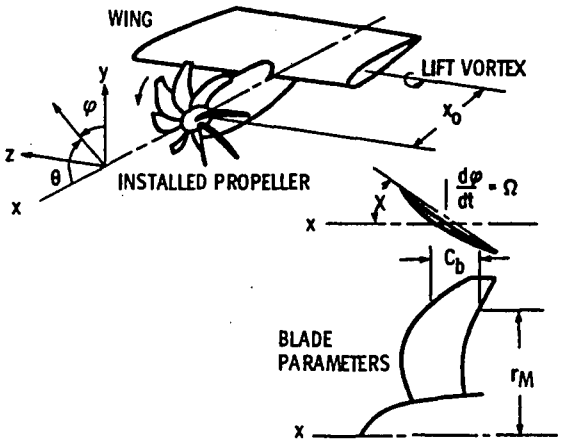

Figure 1. - Defining sketch for installed turboprop.

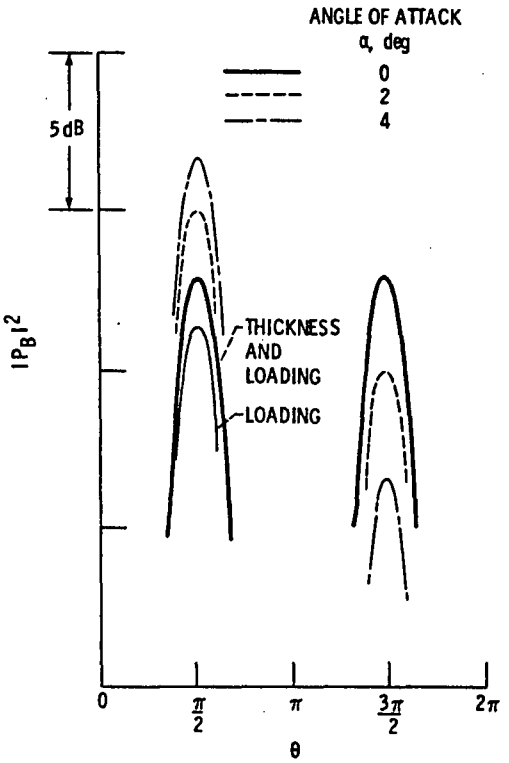

Figure 2. - Effect of propeller angle of attack on fundamental tone directivity in the horizontal plane, $\varphi = \pm \pi/2$.

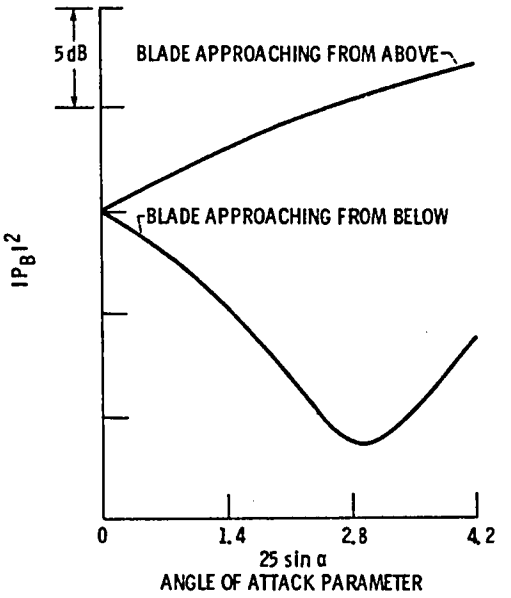

Figure 3. - Effect of propeller angle of attack parameter on fundamental tone peak.

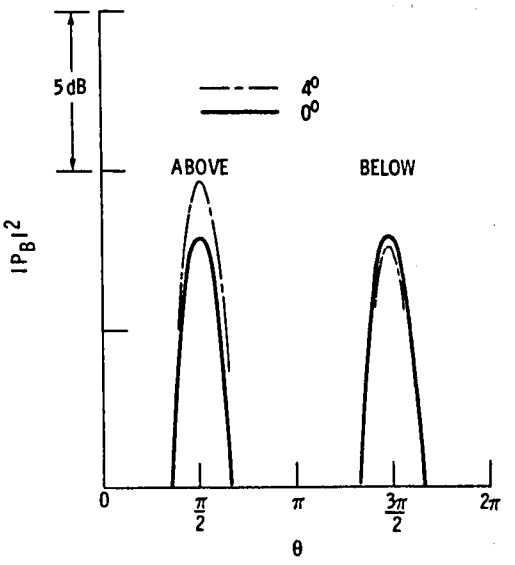

Figure 4. - Effect of propeller angle of attack on fundamental tone directivity in the vertical plane, $\varphi = 0, \pi$.

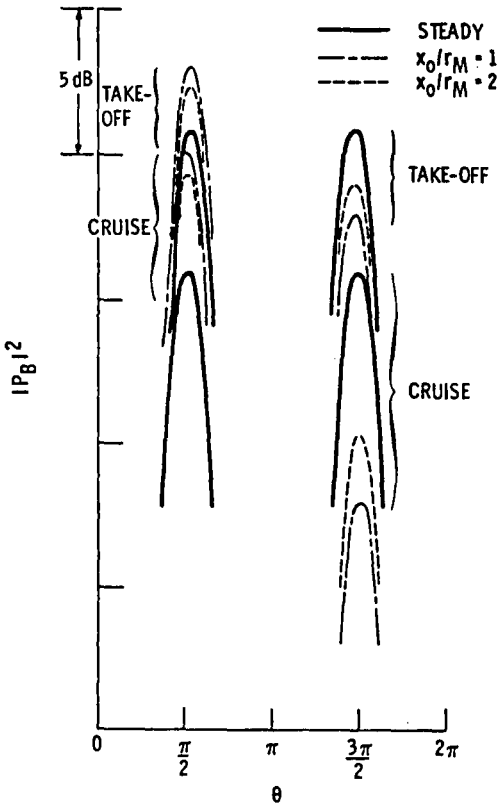

Figure 5. - Effect of wing induced flow non-uniformity on propeller fundamental tone directivity, $\varphi = \pm \pi/2$.

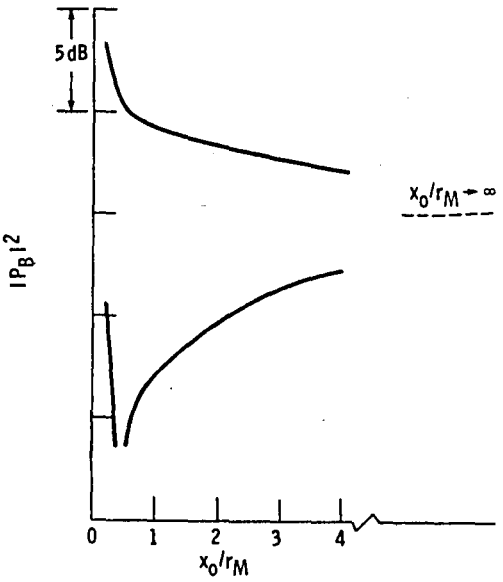

Figure 6. - Dependence of peak noise levels in horizontal plane on distance of prop from center of lift, x_0/r_M, cruise conditions.

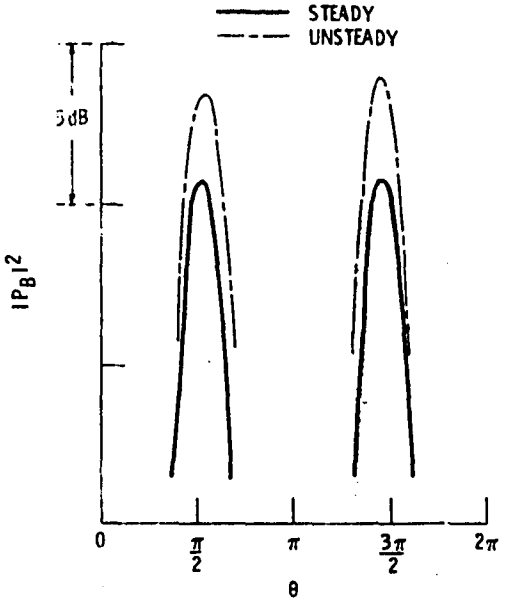

Figure 7. - Vertical plane directivities for take-off situations $x_0/r_M = 1$ and $\varphi = 0, \pi$.

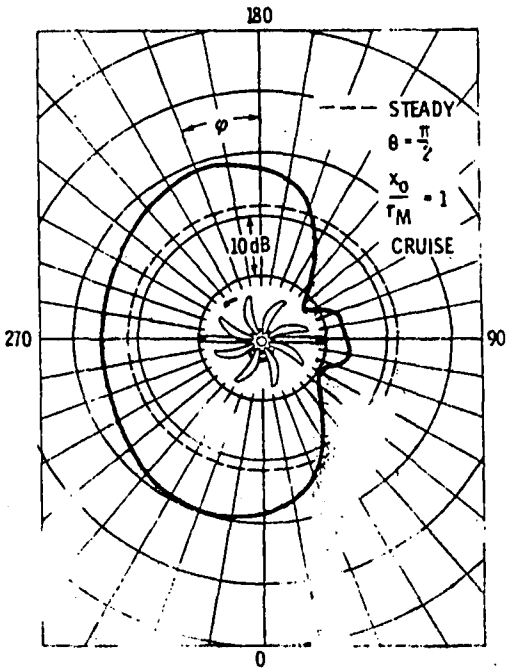

Figure 8. - Directivity of the fundamental tone in the plane of the propeller.

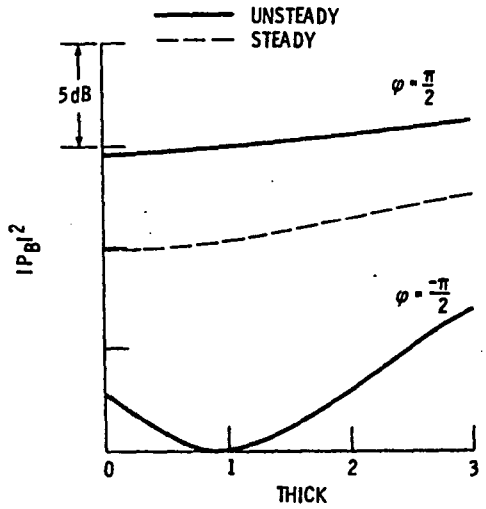

(a) Thickness parameter for cruise conditions. Curves for unsteady noise at $\varphi = \pi/2$ and $-\pi/2$; for steady noise alone $x_0/r_M = 1$.

Figure 9. - Parametric variation of peak noise levels.

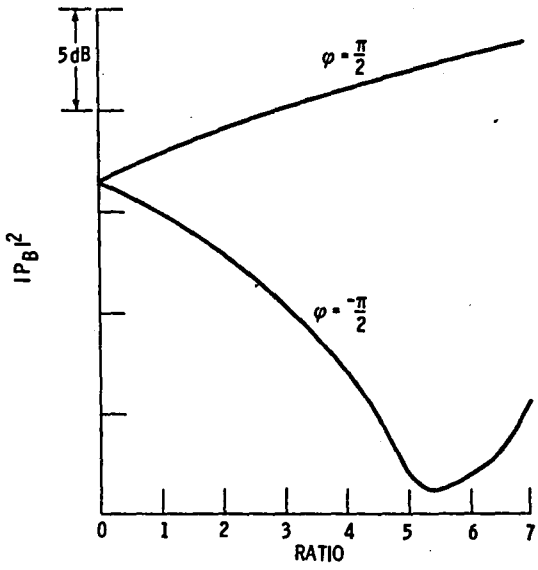

(b) Unsteady to steady thrust factor. Cruise conditions, $\varphi = \pm \pi/2$ and $x_0/r_M = 1$.

Figure 9. - Concluded.

1. Report No. NASA TM-82924	2. Government Accession No.	3. Recipient's Catalog No.
4. Title and Subtitle ROUGH ANALYSIS OF INSTALLATION EFFECTS ON TURBOPROP NOISE		5. Report Date 6. Performing Organization Code 505-32-02
7. Author(s) Paul A. Durbin and John F. Groeneweg		8. Performing Organization Report No. E-1316 10. Work Unit No.
9. Performing Organization Name and Address National Aeronautics and Space Administration Lewis Research Center Cleveland, Ohio 44135		11. Contract or Grant No. 13. Type of Report and Period Covered Technical Memorandum
12. Sponsoring Agency Name and Address National Aeronautics and Space Administration Washington, D. C. 20546		14. Sponsoring Agency Code

15. Supplementary Notes
Prepared for the One hundred fourth Meeting of the Acoustical Society of America, Orlando, Florida, November 8-12, 1982.

16. Abstract

A rough analysis of noise from a propeller operated at angle of attack, and in the nonuniform flow due to a line vortex approximating a wing flow field suggests installation can significantly affect turboprop noise levels. On one side of the propeller, where the blades approach the horizontal plane from above, decreases of noise occur; while on the other side noise increases. The noise reduction is due to negative interference of steady and unsteady sources. An angle of attack, or distance between propeller and vortex, exists for which noise is a minimum.

17. Key Words (Suggested by Author(s))	18. Distribution Statement
Turboprop Noise Unsteady loading	Unclassified - unlimited STAR Category 71

19. Security Classif. (of this report)	20. Security Classif. (of this page)	21. No. of Pages	22. Price*
Unclassified	Unclassified		

* For sale by the National Technical Information Service, Springfield, Virginia 22161

End of Document